AD-A065 075 UNITED TECHNOLOGIES RESEARCH CENTER EAST HARTFORD CONN F/G 21/5
NONLINEAR STOCHASTIC CONTROL DESIGN FOR GAS TURBINE ENGINES.(U)
JUN 78 F A FARRAR, G J MICHAEL N00014-76-C-0710
UNCLASSIFIED UTRC/R78-942577-13 ONR-CR215-247-2F NL

1 OF 1
AD A065075

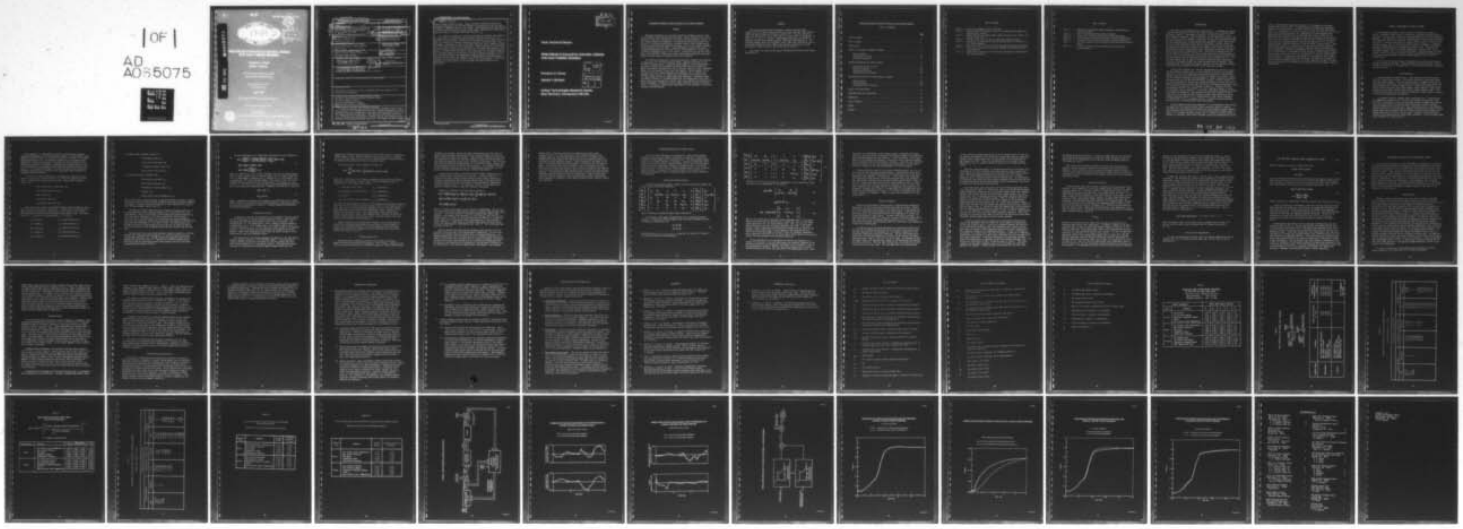

END
DATE FILMED
4 -79
DDC

LEVEL II

REPORT ONR-CR215-247-2F

(12)

OFFICE OF NAVAL RESEARCH

NONLINEAR STOCHASTIC CONTROL DESIGN FOR GAS TURBINE ENGINES

FLORENCE A. FARRAR
GERALD J. MICHAEL

UNITED TECHNOLOGIES RESEARCH CENTER
EAST HARTFORD, CONNECTICUT 06108

CONTRACT N00014-75-C-0710
ONR TASK 215-247

JUNE 1978

FINAL REPORT FOR PERIOD 1 APRIL 1975—31 MARCH 1978

Unclassified

SECURITY CLASSIFICATION OF THIS PAGE (When Data Entered)

REPORT DOCUMENTATION PAGE

READ INSTRUCTIONS BEFORE COMPLETING FORM

1. REPORT NUMBER: ONR-CR215-247-2F	2. GOVT ACCESSION NO.
3. RECIPIENT'S CATALOG NUMBER	
4. TITLE (and Subtitle): NONLINEAR STOCHASTIC CONTROL DESIGN FOR GAS TURBINE ENGINES	5. TYPE OF REPORT & PERIOD COVERED: Final Technical Report, 1 April 1976-31 March 1978
6. PERFORMING ORG. REPORT NUMBER: R78-942577-13	
7. AUTHOR(s): Florence A. Farrar, Gerald J. Michael	8. CONTRACT OR GRANT NUMBER(s): N00014-76-C-0710
9. PERFORMING ORGANIZATION NAME AND ADDRESS: United Technologies Research Center, Silver Lane, East Hartford, Connecticut 06108	10. PROGRAM ELEMENT, PROJECT, TASK AREA & WORK UNIT NUMBERS: 61153N RR014-11-84; NR215-247
11. CONTROLLING OFFICE NAME AND ADDRESS: Office of Naval Research (Code 211), 800 North Quincy Street, Arlington, Virginia 22217	12. REPORT DATE: June 1978; NUMBER OF PAGES: 45
14. MONITORING AGENCY NAME & ADDRESS (if different from Controlling Office)	15. SECURITY CLASS. (of this report): Unclassified
	15a. DECLASSIFICATION/DOWNGRADING SCHEDULE

16. DISTRIBUTION STATEMENT (of this Report)

Approved for public release; distribution unlimited.

17. DISTRIBUTION STATEMENT (of the abstract entered in Block 20, if different from Report)

18. SUPPLEMENTARY NOTES

Reproduction in whole or in part is permitted for any purpose of the United States Government.

19. KEY WORDS (Continue on reverse side if necessary and identify by block number)

Stochastic Nonlinear Multivariable Feedback Control
Gas Turbine Engine Control
Nonlinear Deterministic Control
Nonlinear Multivariable Estimation

20. ABSTRACT (Continue on reverse side if necessary and identify by block number)

Synthesis procedures for nonlinear stochastic feedback control of gas turbine engines were developed and evaluated. Modern estimation and control procedures based upon separating the stochastic and deterministic aspects of the control problem were employed. The resulting closed-loop control consists of (1) nonlinear deterministic feedback control logic designed using piecewise-linear/piecewise-optimal techniques, and (2) an estimator designed

→ next page (over)

DD FORM 1 JAN 73 1473 EDITION OF 1 NOV 65 IS OBSOLETE

S/N 0102-LF-014-6601

409 252

Unclassified

SECURITY CLASSIFICATION OF THIS PAGE (When Data Entered)

20. ABSTRACT (cont'd)

using nonlinear filtering logic. Engine variables estimated from noise-corrupted measurements are fed back through the deterministic control logic to generate commanded inputs to the engine. Mode-switching logic was developed to provide smooth transition between small-signal regulation and large-signal transient modes of estimator/controller operation.

The combined deterministic controller/stochastic estimator was evaluated by application to a nonlinear digital dynamic computer simulation of the F100/F401 turbofan engine. Stability-in-the-large as well as stability-in-the-small at design and off-design operating conditions was established. Engine performance throughout the idle to military sea-level static operating regime (9 to 100 percent thrust) was investigated. Thrust response of the nonlinear F100/F401 engine simulation was evaluated for (1) nominal and degraded engine models, (2) nominal and off-nominal noise statistics and (3) small-signal as well as large-signal time responses. Stochastic engine performance (feedback of estimated measurable and unmeasurable engine variables through the deterministic control logic) was compared with deterministic engine performance (feedback of actual engine variables through the control logic). In addition, computational requirements of the nonlinear controller/estimator were delineated.

Final Technical Report

NONLINEAR STOCHASTIC CONTROL DESIGN FOR GAS TURBINE ENGINES

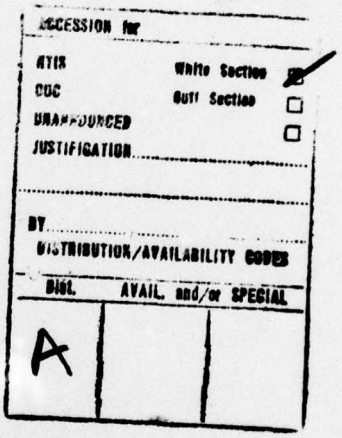

Florence A. Farrar

Gerald J. Michael

United Technologies Research Center
East Hartford, Connecticut 06108

78-05-78-2

Nonlinear Stochastic Control Design for Gas Turbine Engines

SUMMARY

Synthesis procedures for nonlinear stochastic feedback control of gas turbine engines were developed and evaluated. Modern estimation and control procedures based upon separating the stochastic and deterministic aspects of the control problem were employed. The resulting closed-loop control consists of (1) nonlinear deterministic feedback control logic designed using piecewise-linear/piecewise-optimal techniques, and (2) an estimator designed using nonlinear filtering logic. Engine variables estimated from noise-corrupted measurements are fed back through the deterministic control logic to generate commanded inputs to the engine. Mode-switching logic was developed to provide smooth transition between small-signal regulation and large-signal transient modes of estimator/controller operation.

The combined deterministic controller/stochastic estimator was evaluated by application to a nonlinear digital dynamic computer simulation of the F100/F401 turbofan engine. Stability-in-the-large as well as stability-in-the-small at design and off-design operating conditions was established. Engine performance throughout the idle to military sea-level static operating regime (9 to 100 percent thrust) was investigated. Thrust response of the nonlinear F100/F401 engine simulation was evaluated for (1) nominal and degraded engine models, (2) nominal and off-nominal noise statistics and (3) small-signal as well as large-signal time responses. Stochastic engine performance (feedback of estimated measurable and unmeasurable engine variables through the deterministic control logic) was compared with deterministic engine performance (feedback of actual engine variables through the control logic). In addition, computational requirements of the nonlinear controller/estimator were delineated.

FOREWORD

This final technical report documents research performed from 1 April 1977 to 31 March 1978 under Office of Naval Research (ONR) Contract N00014-76-C-0710, Contract Authorization NR215-247. Research performed under this ONR contract from 1 April 1976 to 31 March 1977 is documented in: Farrar, F. A. and G. J. Michael: Large-Signal Estimation for Stochastic Nonlinear Multivariable Dynamic Systems, ONR Report ONR-CR215-247-1. The research program, which was initiated 1 April 1976, was conducted at United Technologies Research Center (UTRC), East Hartford, Connecticut, 06108. Mr. David S. Siegel served as the ONR Scientific Officer.

This report is issued as ONR Report ONR-CR215-247-2F and as UTRC Report R78-942577-13.

Nonlinear Stochastic Control Design for Gas Turbine Engines

TABLE OF CONTENTS

LIST OF FIGURES

LIST OF TABLES

INTRODUCTION

The Naval Air Development Center study of Ref. 1 -- dealing with dynamic response requirements for V/STOL lift/cruise engines used to provide height and moment control -- highlights a problem of increasing concern to the Naval aviation community. This study points out the inability of present day gas turbine lift/cruise engines -- when used directly for differential moment and force generation -- to meet acceleration and height control requirements of V/STOL Flying Qualities Specification MIL-F-83300. Current control of jet-lift V/STOL aircraft at hover and low speeds is therefore accomplished by employing an auxiliary reaction control system which diverts a portion of main engine airflow to the aircraft outer extremities to generate the appropriate flight control moments and forces. Hover and low speed control is accomplished by modulation of airflow nozzles which can be rapidly opened or closed. This mode of auxiliary control results in increased aircraft weight and complexity as well as decreased internal volume available for fuel. If the main engines could be used to provide the required rapid acceleration directly, considerable weight and volume savings would be realized. These considerations will assume even greater importance in the future as the Navy progresses with development of V/STOL A and B aircraft concepts.

Previous UTRC programs with ONR have demonstrated the ability of multivariable feedback control logic -- using feedback of actual, not estimated, variables -- to provide significantly more rapid propulsion system dynamic response than that associated with conventional control logic (Refs. 2 and 3). The Ref. 2 report documents this improvement in dynamic response with particular application to the Navy XFV-12A V/STOL aircraft. Results obtained in a UTRC study supported by the National Science Foundation indicate that use of adaptive multivariable control logic for static performance optimization leads to reduced thrust specific fuel consumption (Ref. 4). However, the UTRC multivariable control logic of Refs. 2, 3 and 4 employs feedback of actual, not estimated, engine variables. In practice, key engine variables are either unavailable for feedback or are measured through noisy, imperfect sensors. A practical design approach must therefore achieve rapid propulsion system response while accounting for (1) unavailability of key output variables, (2) measurement noise, (3) actuator errors, (4) system-to-system parameter variations, and (5) unpredictable plant disturbances.

A design approach based upon separation of the deterministic and stochastic aspects of the control problem offers a potential means for meeting increased Naval requirements associated with rapid propulsion system response. This design procedure involves (1) nonlinear deterministic feedback control design, (2) nonlinear estimator design, and (3) closed-loop control based on feedback of estimated system state variables through the deterministic control

logic. The analytical techniques required for development of nonlinear deterministic control logic -- in particular, piecewise-linear/piecewise-optimal (PLPO) procedures -- have been developed by UTRC under ONR support (Ref. 5). Procedures for nonlinear estimator design using nonlinear filtering logic with PLPO-computed gains and compensation for model-mismatch have been developed and evaluated in an ONR-supported study at UTRC (Ref. 6). Therefore, this research study was directed toward combining the deterministic control and stochastic estimation algorithms and evaluating the resulting closed-loop engine/estimator/controller by application to a nonlinear digital dynamic computer simulation of the F100/F401 turbofan engine. Mode-switching logic was to be developed to provide smooth transition between small-signal regulation and large-signal transient modes of estimator/controller operation. Stability-in-the-large as well as stability-in-the-small was to be determined. Performance of the nonlinear F100/F401 engine simulation/estimator/controller was to be evaluated for (1) nominal and degraded engine models, (2) nominal and off-nominal noise statistics, and (3) small-signal as well as large-signal time responses. An important constraint on the closed-loop estimator/controller to be developed will be that its computational requirements be compatible with projected airborne digital computer capabilities.

CONTROL OF NONLINEAR STOCHASTIC SYSTEMS

The nonlinear stochastic control problem is presented in detail in Ref. 6. Reference 6 sets forth (1) the general nonlinear stochastic system structure, (2) the control objectives and constraints, and (3) the UTRC design approach. This approach is based upon separating the stochastic and deterministic aspects of the control problem. The stochastic control design procedure involves (1) nonlinear deterministic feedback control design, (2) nonlinear estimator design, and (3) closed-loop control based on feedback of estimated engine variables through the deterministic control logic. The analytical techniques for defining the nonlinear deterministic control (Ref. 5) and nonlinear estimator (Ref. 6) have been developed. These techniques for deterministic control design and estimator design were evaluated by application to a nonlinear digital dynamic F100/F401 engine simulation (Refs. 3 and 6, respectively).

In this section the procedures for deterministic control and stochastic estimator design are reviewed. Engine dynamics are described first. Deterministic control logic is discussed next. The stochastic estimation algorithm is then set forth.

Engine Dynamics

The system model is shown in Fig. 1 with provision for the estimation and control algorithms included. The system consists of a nonlinear engine model and sensor models. Fuel flow driving noise is included to account for metering valve uncertainty. Engine state variables are generated through the engine dynamics and the actual engine inputs. These state variables in conjunction with the actual inputs govern engine output response. Engine state variables are available through sensors which contain inherent lags. These sensors indicate which state variables are measured. Sensor noise is included to account for measurement inaccuracies.

A nonlinear F100/F401 turbofan engine simulation (Ref. 7) was selected for comparative evaluation of the control and estimation algorithms. The F100/F401 afterburning turbofan is a military propulsion system incorporating the latest achievements of advanced engine technology including variable control geometries and digital electronic supervisory control. The variable geometries as well as the nonlinear, complex, multivariable interactions among engine input-output variables make the F100/F401 engine a particularly challenging application of modern control theory. Dynamics of this nonlinear simulation are represented by sixteen state variables. A set of sixteen engine state variables is listed in Ref. 6.

The complexity of a deterministic control and stochastic estimator designed using modern control and estimation theory -- in particular, linear quadratic Gaussian theory -- is directly related to the order of the linear engine design model (i.e., the number of states used in the engine model employed in the design procedure). Including all state variables in the design model results in unnecessary complexity in the design effort as well as in implementation requirements of the resulting combined estimator/controller. It is therefore desirable to reduce the order of the full-state linearized engine model by retaining only significant engine dynamics for estimator/controller design.

The first step toward determining a reduced-order linearized engine model for control and estimator design is to select the engine state variables. A fifth-order design model was chosen. Engine state variables selected are:

- fan turbine inlet temperature (x_1)
- main burner pressure (x_2)
- fan speed (x_3)
- compressor speed (x_4)
- afterburner pressure (x_5).

These five engine states are available through sensors modeled by first-order lags and noise sources. Therefore, in addition to the five selected engine states there are five sensed states -- the outputs of the sensors. The measurements represent noise-corrupted sensed engine states. The sensed states $x_6 \ldots x_{10}$ and noisy measurements $z_1 \ldots z_5$ are:

x_6 = sensed x_1	z_1 = noise-corrupted x_6
x_7 = sensed x_2	z_2 = noise-corrupted x_7
x_8 = sensed x_3	z_3 = noise-corrupted x_8
x_9 = sensed x_4	z_4 = noise-corrupted x_9
x_{10} = sensed x_5	z_5 = noise-corrupted x_{10}.

The engine input variables chosen are:

- jet exhaust area (u_1)
- fan inlet guide vanes (u_2)
- compressor variable vanes (u_3)
- main burner fuel flow (u_4).

Critical engine output variables are:

- fan corrected airflow (y_1)
- fan stability margin (y_2)
- compressor stability margin (y_3)
- thrust (y_4)
- high turbine inlet temperature (y_5).

These engine output variables cannot be measured directly in flight. However, the time evolution of these critical variables determines satisfactory engine performance. Accurate in-flight estimation of these variables will lead to more effective dynamic control (Ref. 8).

Deterministic control and stochastic estimation throughout the idle to military sea-level static operating regime (9 to 100 percent thrust) was investigated. Table I lists values of the steady-state engine variables for sea-level static conditions at five power lever angle (PLA) settings: PLA = 20, 35, 47, 60 and 73 deg. For convenience, all engine parameters except fan and compressor vane positions and fan and compressor stability margins have been normalized to 1.0 at PLA = 73 deg. The vane positions are defined as ratios of their maximum positions and the two stability margins are given as ratios of one (a smaller value indicates reduced stability margin).

The next step in the control and estimator design procedure is to define reduced-order linearized system dynamics at a series of points along the steady-state operating line. Several methods for computing reduced-order dynamics are described in Ref. 6. Reduced-order F100/F401 engine models were calculated by identifying reduced-order dynamics directly from input-output-state data (Refs. 5 and 9).

Linearized dynamics at a steady-state operating point are represented by

$$\delta\dot{x}(t) = \begin{bmatrix} \delta\dot{x}_e(t) \\ \hline \delta\dot{x}_s(t) \end{bmatrix} = \left[\begin{array}{c|c} A_e & O_{5,5} \\ \hline A_\tau & -A_\tau \end{array}\right] \begin{bmatrix} \delta x_e(t) \\ \hline \delta x_s(t) \end{bmatrix} + \begin{bmatrix} B_e \\ \hline O_{5,4} \end{bmatrix} \left[\delta u(t) + \xi(t)\right]$$

$$\delta y(t) = C\delta x_e(t) + D(\delta u(t) + \xi(t)) \qquad (1)$$

$$\delta z(t) = \left[O_1' I_5\right] \begin{bmatrix} \delta x_e(t) \\ \hline \delta x_s(t) \end{bmatrix} + \eta(t)$$

where the vectors x_e, x_s, u, y, and z represent the five (5) engine states, five (5) sensor states, four (4) engine inputs, five (5) engine outputs and five (5) measurements, respectively, O_{ij} denotes an i x j null matrix, and I_j represents a j^{th} order identity matrix. The vectors ξ (4x1) and η (5x1) represent process and sensor noise, respectively. The constant A_e (5x5), B_e (5x4), C (5x5) and D (5x4) matrices define engine perturbational dynamics about the steady-state operating point. Elements of the matrix A_τ (5x5) are

$$(A_\tau)_{ij} = \frac{1}{\tau_i}, \; i=j$$

$$(A_\tau)_{ij} = 0, \; i \neq j \qquad (2)$$

where τ_i represents the sensor time constant associated with the i^{th} engine state. Sensor time constants and standard deviations of sensor and fuel flow driving noise are presented in Table II. Variable geometry uncertainties were assumed negligible.

Deterministic Control

A systematic technique for deterministic multivariable nonlinear system control design based on linear quadratic regulator theory -- specifically, the piecewise-linear/piecewise-optimal (PLPO) control technique -- was developed (Ref. 5). The deterministic control design procedure assumes no uncertainities; i.e., it is assumed that (1) no actuator errors exist, (2) no plant disturbances occur, (3) all state and output variables are measured perfectly, and (4) actuator and plant dynamics and parameters are known exactly. Under these assumptions, plant state and output variables can be determined for any given commanded inputs.

The deterministic PLPO design procedure was applied to the P&WA digital computer dynamic simulation of the F100/F401 engine. A nonlinear multivariable feedback controller was defined for idle to military sea-level static engine operation (9 to 100 percent thrust). The analytical design involved (1) linearizing the F100/F401 engine dynamics about the five

steady-state operating points between idle and military thrust, (2) applying linear optimal control synthesis methods at each point, and (3) combining the five optimal linear controllers into a single nonlinear controller which had feedback gains scheduled with high compressor speed.

The deterministic control dynamics are given by

$$u(t) = \int_{x_e(0)}^{x_e(t)} L(N_2)\, dx_e(\tau) + \int_0^t H(N_2)(v(\tau) - v_c(\tau))\, d\tau + u(0) \qquad (3)$$

where the L (4x5) and H (4x4) matrices represent proportional plus integral feedback controller gains, respectively. The high compressor speed is denoted by N_2. The vectors v and v_c are:

v_1 = fan inlet guide vanes	v_{c1} = commanded v_1
v_2 = compressor variable vanes	v_{c2} = commanded v_2
v_3 = thrust	v_{c3} = commanded v_3
v_4 = high turbine inlet temperature	v_{c4} = commanded v_4.

The controller gain matrices, L and H, at the steady-state operating conditions (PLA = 20, 35, 47, 60 and 73 deg) are listed in Ref. 3. Note from v_3 and v_4 above that this control mode requires feedback of thrust and high turbine inlet temperature -- two of the five unmeasurable output variables -- in addition to the engine states. Also, engine states are available only through noise-corrupted sensors with inherent lags. However, in the deterministic control study, engine states, thrust, and high turbine inlet temperature were assumed to be known exactly.

Results obtained in the deterministic dynamic control study indicate the ability of multivariable feedback control logic -- using feedback of actual, not estimated, variables -- to provide significantly more rapid propulsion system dynamic response than that associated with conventional control logic (Refs. 2 and 3).

Estimation Algorithm

State and output estimation procedures for stochastic nonlinear dynamic systems were developed and evaluated. The stochastic aspects of the problem are reintroduced for this estimation portion of control system design.

In addition to process, sensor, and model uncertainties, the fact that all engine variables cannot be measured and that any measurement is subject to sensor errors was taken into account. Model-mismatch compensation techniques were employed to account for potential mismatch between the system model in the filtering algorithm and the actual nonlinear system model. The filtering algorithm was evaluated by application to the nonlinear digital dynamic computer simulation of the F100/F401 turbofan engine. An important constraint on the estimation algorithm is that its computational requirements be compatible with projected airborne digital computer capabilities.

A large-signal estimation algorithm based on Kalman estimation theory with model-mismatch compensation was developed. Results obtained in a previous UTRC study directed toward stochastic small-signal regulation of nonlinear multivariable dynamic systems indicate that to achieve accurate estimation Kalman filtering methodology with model-mismatch compensation should be employed (Ref. 8). In addition, the Ref. 8 study showed that improved estimation leads to improved stochastic regulation.

Dynamics of nonlinear filtering logic are given by

$$\dot{\hat{x}}_e(t) = f_1(\hat{x}_e^+(t), u(t), 0) + K_{f_1}(\hat{N}_2)(z(t) - \hat{x}_s(t)) + \int_0^t K_c(\hat{N}_2)(z(\tau) - \hat{x}_s(\tau))\,d\tau$$

$$\dot{\hat{x}}_s(t) = A_\tau(\hat{x}_e(t) - \hat{x}_s(t)) + K_{f_2}(\hat{N}_2)(z(t) - \hat{x}_s(t)) \qquad (4)$$

$$\hat{y}(t) = g(\hat{x}_e^+(t), u(t), 0)$$

where $(\hat{\ })$ denotes the estimate of the variable in parentheses. The x_e^+ notation denotes full-state representation whereas x_e denotes reduced-state representation. The vector function f represents reduced-order engine state dynamics. The Kalman filter matrices, K_{f_1} (5x5) and K_{f_2} (5x5), and the compensator gains, K_c (5x5), are calculated off-line at the five (5) operating points based on the fifth-order linear representations of the nonlinear engine simulation. These gains are computed using Kalman filtering theory as well as model-mismatch compensation logic (Ref. 6). The filter gains are tabulated in Ref. 6.

Results obtained show that precise estimation was achieved using the nonlinear filtering logic with model-mismatch compensation. Accurate estimation of key engine states and outputs from (1) nominal-engine data, (2) degraded-engine data, and (3) engine data with off-nominal noise statistics (that is, noise statistics different from the statistics assumed in calculating the filter gains) was obtained with the nonlinear filtering algorithm. In addition, the computational requirements of the nonlinear filtering logic are significantly less than the computational requirements of an extended

Kalman filter. The major reduction in computation is due to gain calculation (Ref. 6). Gain calculation for an extended Kalman filter designed using the reduced-order engine model and not including on-line linearization would require 5325 multiplications per sampling interval and 4885 additions per sampling interval. These computations are based on ten states (five engine and five sensed states), four inputs, and five measurements. On the other hand, gain calculation for the nonlinear filtering algorithm for the sea-level static flight condition considered here requires only 75 multiplications per sampling interval and 150 additions per sampling interval. Including sensor model mismatch would increase the required multiplications and additions by 25 and 50, respectively. These results imply that the nonlinear estimation logic described here provides a potentially viable approach to estimation of key engine variables under realistic operating conditions.

COMBINED ESTIMATION AND CONTROL DESIGN

In this section combining the deterministic control and stochastic estimator into a unified feedback controller is presented. Closed-loop linearized system dynamics are introduced first. The relationship between control and estimator dynamics is discussed. Assessing closed-loop system stability is then set forth. Mode-switching logic to achieve rapid small-signal as well as large-signal response is described next. Also, mode-switching logic to achieve rapid, stable degraded engine as well as nominal engine response is discussed. In the final part of this section computational requirements for the combined estimation and control algorithm are delineated.

Closed-Loop System Dynamics

Closed-loop linearized engine, sensor, filter, and control dynamics are given by the differential equations

$$\begin{bmatrix} \delta\dot{x}_e \\ \delta\dot{u} \\ \delta\dot{x}_s \\ \delta\dot{\hat{x}}_e \\ \delta\dot{\hat{x}}_s \\ \delta\dot{\hat{w}} \end{bmatrix} = \begin{bmatrix} A_e & B_e & 0 & 0 & 0 & 0 \\ 0 & HD_e+LB_e & LK_{f_1} & HC_e+LA_e & -LK_{f_1} & L \\ A_\tau & 0 & -A_\tau & 0 & 0 & 0 \\ 0 & B_e & K_{f_1} & A_e & -K_{f_1} & I \\ 0 & 0 & K_{f_2} & A_\tau & -K_{f_2}-A_\tau & 0 \\ 0 & 0 & K_c & 0 & -K_c & 0 \end{bmatrix} \begin{bmatrix} \delta x_e \\ \delta u \\ \delta x_s \\ \delta\hat{x}_e \\ \delta\hat{x}_s \\ \delta\hat{w} \end{bmatrix} + \begin{bmatrix} B_e\xi \\ LK_{f_1}\eta - H\delta v_c \\ 0 \\ K_{f_1}\eta \\ K_{f_2}\eta \\ K_c\eta \end{bmatrix} \quad (5)$$

where w represents linearized engine model uncertainty.

An alternate state-space representation of the closed-loop system dynamics is obtained by defining engine state and sensor estimation errors (e_1 and e_2), respectively, by

$$\begin{aligned} e_1 &= x_e - \hat{x}_e \\ e_2 &= x_s - \hat{x}_s . \end{aligned} \quad (6)$$

Substituting $\hat{x}_e = x_e - e_1$, $\hat{x}_s = x_s - e_2$ from Eq. (6) into Eq. (5) leads to closed-loop linearized system dynamics

$$\begin{bmatrix} \delta\dot{x}_e \\ \delta\dot{u} \\ \delta\dot{x}_s \\ \delta\dot{e}_1 \\ \delta\dot{e}_2 \\ \delta\dot{\hat{w}} \end{bmatrix} = \left[\begin{array}{cc|c|ccc} A_e & B_e & 0 & 0 & 0 & 0 \\ LA_e+HC_e & LB_e+HD_e & 0 & -(LA_e+HC_e) & LK_{f_1} & L \\ \hline A_T & 0 & -A_T & 0 & 0 & 0 \\ \hline 0 & 0 & 0 & A_e & -K_{f_1} & -I \\ 0 & 0 & 0 & A_T & -(A_T+K_{f_2}) & 0 \\ 0 & 0 & 0 & 0 & K_c & 0 \end{array}\right] \begin{bmatrix} \delta x_e \\ \delta u \\ \delta x_s \\ \delta e_1 \\ \delta e_2 \\ \delta\hat{w} \end{bmatrix} + \begin{bmatrix} B_e\xi \\ LK_{f_1}\eta - H\delta v_c \\ 0 \\ B_e\xi - K_{f_1}\eta \\ -K_{f_2}\eta \\ K_c\eta \end{bmatrix}. \tag{7}$$

From Eq. (7) it can be seen that the eigenvalues of the closed-loop system are given by the eigenvalues of the matrices

$$F_{11}(9\times 9) \triangleq \begin{bmatrix} A_e & B_e \\ LA_e+HC_e & LB_e+HD_e \end{bmatrix}, \tag{8}$$

$$F_{22}(5\times 5) \triangleq -A_T, \tag{9}$$

$$\text{and} \quad F_{33}(15\times 15) \triangleq \begin{bmatrix} A_e & -K_{f_1} & -I \\ A_T & -(A_T+K_{f_2}) & 0 \\ 0 & K_c & 0 \end{bmatrix}. \tag{10}$$

That is, the closed-loop linearized system eigenvalues are (1) the eigenvalues associated with the deterministic control (Eq. (8)), (2) the eigenvalues associated with the sensor dynamics (Eq. (9)), and (3) the eigenvalues associated with the stochastic estimator (Eq. (10)). The deterministic control eigenvalues can therefore be adjusted by the value of the feedback control gains H and L (which depend on the weighting matrices within the control performance criterion) while the estimator eigenvalues can be adjusted by the value of the filter gains (which depend on the process, sensor, and model-mismatch noise intensity matrices).

If the eigenvalues of the deterministic control are dominant (i.e., closer to the $j\omega$ axis in the left half plane) the transient response of the closed-loop system in the stochastic environment will be similar to that of the deterministic response. However, the system response will be noise-corrupted because the filter will pass much of the measurement noise. This

noise acts as a disturbance on the control system. Designing the filter/control so that the control eigenvalues are dominant appears to be applicable only when measurements are very accurate. On the other hand, if the eigenvalues of the estimator are dominant, closed-loop system transient response will be different from the deterministic response. Therefore, the controller should be designed so that the estimator and deterministic control eigenvalues are similar if the system measurements are noise-corrupted.

Filter and control gains at five design operating points (PLA = 20, 35, 47, 60 and 73 deg) were calculated previously. Model-mismatch uncertainty was selected in the estimator design so that neither the control nor filter eigenvalues were dominant. Error indices -- which measure the normalized root mean-square error between linear and nonlinear model time responses -- were employed as a measure of the linearized model uncertainties. Table III lists the eigenvalues associated with the sensor dynamics, with the deterministic control, and with the stochastic estimator at PLA = 73 deg. This table indicates that the magnitudes of the eigenvalues associated with the stochastic estimator are similar to the magnitudes of the eigenvalues associated with the deterministic control, i.e., neither the estimator nor controller dynamics are dominant. Similar results were obtained at the other design points.

Stability Analysis

Stability-in-the-small at design points is assured under appropriate assumptions for filter and control design using PLPO techniques. Closed-loop system stability-in-the-small at off-design points is not guaranteed due to the interpolation of estimator and control gains. Stability at the off-design points was determined directly from computation of closed-loop system eigenvalues at those points. To assess stability-in-the-small at off-design operating points (1) open-loop linearized F100/F401 engine models were identified at the off-design operating points, and (2) closed-loop stability-in-the-small was determined from the linear models with appropriate control and estimator gains.

To identify open-loop linearized models for determining stability-in-the-small at off-design operating points deterministic input-output-state data were generated by the nonlinear F100/F401 engine simulation at four off-design steady-state operating conditions. The four off-design operating points selected were midway as a function of PLA between the design operating points (that is, PLA = 28, 41, 54, 67 deg). To generate the data the engine inputs were sequentially stepped at the steady-state off-design operating conditions. The step input duration was one second with one-half second between the input steps. The step magnitudes were approximately

(1) five percent military operating point on jet exhaust area, (2) five and ten percent of maximum position on fan inlet guide vanes and rear compressor variable vanes, respectively, and (3) five percent of operating point on main burner fuel flow. These input perturbations are the same as those perturbations used to identify linearized models at the design operating points.

Open-loop linearized models for determining stability-in-the-small were identified at the four off-design operating conditions from deterministic input-output-state data generated by the nonlinear F100/F401 engine simulation. The least-squares identification technique was used to compute parameters of the linearized models from this engine data. The combination of sequential step inputs and least-squares parameter identification has been an effective approach for defining credible linear system models from noise-free data when all variables are available.

State and output error indices at the four off-design operating conditions are listed in Table IV. These error indices are normalized root-mean-square differences between actual and calculated engine model time responses. Previous UTRC studies indicate that identified engine dynamics with error indices less than 0.5 adequately predict small-signal nonlinear engine performance for control and estimator design. Table IV indicates that error indices associated with the identified linear models at the off-design operating points are much smaller than 0.5. Actual and identified engine model state responses with the largest and smallest error indices at PLA = 67 deg are shown in Fig. 2. Actual and identified engine model output responses with the largest and smallest error indices at PLA = 67 deg are compared in Fig. 3. The comparison of engine responses at PLA = 67 deg is representative of results at the other three off-design operating conditions. These time responses in conjunction with Table IV show that the identified linear models accurately predict small-signal nonlinear engine response.

Closed-loop stability-in-the-small at the off-design operating conditions was determined from the identified linear models with appropriate control and estimator gains. Control and estimator feedback gain matrices at the off-design operating points were determined from control and estimator gains at adjacent design operating points using linear interpolation with compressor speed as the independent variable. (Linear interpolation is employed to schedule filter and control gains as a function of compressor speed within the stochastic control logic interfaced with the nonlinear F100/F401 engine simulation.) Stability-in-the-small at off-design operating points was demonstrated by computing closed-loop system eigenvalues (Eq. (7)). Closed-loop eigenvalues at PLA = 67 deg are shown in Table V. This table indicates the desirable situation where neither estimator nor controller dynamics are dominant. Similar results were obtained at the other three

off-design operating conditions. In addition, magnitudes of the eigenvalues at off-design operating points are of the same order of magnitude as the magnitudes of the eigenvalues at the adjacent design operating conditions (see Tables III and V).

The control and estimator synthesis procedure using the separation approach does not guarantee stability-in-the-large for nonlinear system dynamics. Stability-in-the-large was assessed through computer simulation. Combined engine simulation/sensor models/control logic/ estimation algorithm performance as well as stability-in-the-large is described in the performance evaluation section.

Mode-Switching Logic

Mode-switching logic was developed to provide rapid small-signal thrust response. The deterministic controller feedback gains, optimized for large-signal response, are, in essence, "tuned" to large initial errors between commanded and actual engine variables. When these errors are small -- as in small-signal transient response -- these deterministic control gains are too small to provide rapid small-signal response. To obtain rapid small-signal as well as rapid large-signal dynamic response mode-switching logic was developed. The mode-switching logic amplifies the commanded engine variable errors (differences between estimated and commanded engine variables which drive the deterministic control integral path). These errors are amplified when the thrust error is small and the high turbine inlet temperature is not near its maximum limit. The amplification gain which multiplies the commanded engine variable errors is given by

$$K = K_1 K_2 \tag{11}$$

where K_1 is a function of the thrust error and K_2 is a function of the estimated high turbine inlet temperature. A schematic diagram of the mode-switching logic to achieve rapid small-signal response is depicted in Fig. 4. Figure 4 shows that for estimated high turbine inlet temperatures less than 50 percent military operating condition K_2 is equal to 1.0 and the amplification gain is a function of the thrust error only (i.e., $K = K_1$). For estimated high turbine inlet temperatures greater than or equal to 75 percent military operating condition (military operating condition represents the maximum temperature operating limit), K_2 is equal to the inverse of K_1 and K is equal to 1.0. That is, when the high turbine inlet temperature is at or above 75 percent of its safe steady-state operating condition the errors are not amplified. For temperatures between 50 and 75 percent K_2 varies smoothly

between 1.0 and the inverse of K_1 and K varies smoothly between K_1 and 1.0. The gain K_1 was defined as a function of the thrust error, as shown in Fig. 4, to insure smooth transition between small-signal and large-signal modes. If the thrust error is greater than 10 percent military thrust, then K = 1.0, K_2 = 1.0 and the errors to the controller are not amplified. For thrust errors ranging from 10 percent to 5 percent K_1 varies linearly from 1.0 to 25.0. When the thrust error is less than 5 percent, K_1 = 25.0. The slopes of K_1 and K_2 as well as the maximum value for K_1 were chosen to yield stable, rapid small-signal engine thrust response.

In addition, logic was developed to achieve stable, rapid degraded engine performance. The deterministic control logic steady-state schedules (requested steady-state thrust, high turbine inlet temperature, fan and compressor vane positions as a function of PLA) are defined for the nominal engine. As the engine degrades these schedules can no longer be achieved. The critical variables in steady-state operation are thrust and high turbine inlet temperature. A degraded engine operating at nominal temperature generally will achieve a thrust less than nominal. In previous UTRC F100 deterministic control studies the deterministic controller provided increased thrust by decreasing area to its lower position limit thereby saturating the area control. When jet exhaust area is unable to recover from saturation unstable engine operation results. To prevent area saturation as steady-state degraded engine operation is reached jet exhaust area is set to its steady-state value (as a function of PLA) as engine operation reaches steady-state. When the absolute value of the thrust error is less than 20 percent military, the normalized area is ramped at 0.5 sec to its steady-state value. That is, jet exhaust area is calculated by

$$A_j(t + \Delta t) = A_j(t) + 0.5\,\Delta t \quad \text{for } |\text{thrust error}| < 0.2. \tag{12}$$

When the absolute value of the thrust error is greater than or equal to 20 percent military thrust then jet exhaust area is computed according to Eq. (3).

Computational Requirements

To code the deterministic control logic on a digital computer the control equation (Eq. (3)) with mode-switching logic (Eq. (11) and Fig. 4) may be represented by

$$u(t+\Delta t) = u(t) + L(N_2(t))\,\Delta x_e(t) + H_c(N_2(t))\,K(v(t) - v_c(t)) \tag{13}$$

where Δt represents the known sampling rate, and

$$\Delta x_e(t) = x_e(t) - x_e(t-\Delta t)$$

$$H_c = H\Delta t \ . \tag{14}$$

Linear univariate interpolation for determining control gains L and H_c between operating points based on $\hat{N}_2$ as well as to compute the mode-switching logic gains K_1 and K_2 as functions of thrust error and high turbine inlet temperature, respectively, is employed in the estimator/controller. That is,

$$g_{ke} = m_i(N_2 - (N_2)_i) + (g_{ke})_i$$

$$m_i = \frac{(g_{ke})_{i+1} - (g_{ke})_i}{(N_2)_{i+1} - (N_2)_i} \tag{15}$$

where i represents a steady-state operating condition and $(N_2)_i \le \hat{N}_2 \le (N_2)_{i+1}$.

Control computational requirements (from Eqs. (13) and (15)) consist of multiplications and additions. To calculate the control and mode-switching logic gains (Eq. (15)) 38 multiplications and 76 additions per sampling interval are required. To calculate updated inputs (Eq. (13)) 41 multiplications and 45 additions per sampling interval are needed. Therefore, the deterministic control with mode-switching logic requires 79 multiplications and 121 additions each sampling interval to compute the engine inputs.

Computational requirements for the nonlinear filtering logic are discussed in detail in Ref. 6. Filter computational requirements depend upon (1) filter gain calculations and (2) the engine model employed in the filter. The gain calculations require only 75 multiplications and 150 additions per sampling interval. These gain calculations are significantly less than those required by the conventional extended Kalman filter (5185 multiplications and 4745 additions per sampling interval.) A minimum complexity nonlinear engine model should be selected for the filtering algorithm to reduce model computational requirements. Results indicate that model-mismatch compensation logic is able to compensate for differences between the engine model employed in the filter and the actual engine. The filter computations (dependent on model used in filter) added to the control computations represent the computations required to implement the nonlinear stochastic control algorithm.

PERFORMANCE EVALUATION OF THE STOCHASTIC CONTROL

In this section stochastic control performance is evaluated. To evaluate closed-loop engine performance including stability-in-the-large the nonlinear F100/F401 engine simulation was interfaced with the nonlinear stochastic feedback control algorithm. The closed-loop engine/stochastic control structure is shown in Fig. 1. The overall closed-loop system consists of (1) the nonlinear F100/F401 engine simulation, (2) sensor models, (3) deterministic PLPO control logic with mode-switching, and (4) nonlinear filtering logic with model-mismatch compensation. The stochastic controller performance when interfaced with a nominal engine is discussed first. Small-signal as well as large-signal response is evaluated. Degraded-engine performance is then described. Engine performance when measurement and fuel flow noise statistics are different from those statistics assumed in estimator design is set forth in the final part of this section.

Nominal Engine

Stochastic engine accelerations from idle (PLA = 20 deg) to military (PLA = 73 deg) thrust levels were computed using the closed-loop nominal nonlinear engine, sensors with the nominal noise statistics, filter, and control. These large-signal accelerations were compared with the deterministic accelerations (nominal engine/controller with no noise and no estimator) of the Ref. 3 study. Results indicate that deterministic and stochastic time responses are almost identical. Stochastic thrust response is compared with the deterministic thrust response in Fig. 5. Figure 5 illustrates that stochastic thrust response for the nominal engine with nominal noise statistics is as rapid as deterministic thrust response. As desired, there is no difference in nominal-engine stochastic and deterministic thrust responses due to the stochastic controller mode-switching logic to accommodate engine degradation. This mode-switching logic was not required in the deterministic control since no uncertainties, including engine degradation, were considered in the deterministic design procedure. The stochastic engine response of the other engine variables was very similar to the deterministic response. The similar stochastic and deterministic engine performance results from the accurate estimation achieved by the nonlinear filtering logic. The mean and standard deviation of state and output estimation errors (where the estimation error $\triangleq$ actual-estimated response) are shown in Table VI. Table VI indicates that the average error is zero to at least three significant figures for all state and output estimates. The maximum standard deviation is 0.002 in fan turbine inlet temperature.

To evaulate closed-loop small-signal system performance stochastic engine response to a PLA step from 20 to 23 deg was generated.

Small-signal actual engine model thrust response using control logic with and without mode-switching logic is compared in Fig. 6. Figure 6 indicates that the small-signal thrust response with mode-switching logic incorporated into the PLPO controller is significantly faster than the thrust response without mode-switching logic. For example, the 11.9 percent thrust point (90 percent of the requested change in thrust) is reached in 3.0 sec using mode-switching logic versus 4.2 sec when mode-switching logic is not employed. Similar rapid small-signal thrust response was achieved using the stochastic controller with mode-switching logic at other off-design as well as design points. Results obtained indicate that (1) the controller requires mode-switching logic to obtain rapid small-signal as well as rapid large-signal dynamic response and (2) mode-switching logic provides smooth transition between the large- and small-signal modes of operation.

Degraded Engine

To evaluate mode-switching control logic developed to accommodate engine degradation, degraded-engine response to a step in PLA from 20 to 73 deg was generated using the stochastic controller without and then with the mode-switching control logic (Eq. (12)). Engine degradation was accomplished by decreasing fan and compressor efficiencies four (4) percent and one (1) percent, respectively. Large-signal engine performance to a step in PLA from 20 to 73 deg was not satisfactory using the controller without mode-switching logic. The thrust did not reach military operation, the fan surged, and the turbine overtemperatured. This poor engine performance results from the fact that steady-state schedules (requested steady-state thrust, high turbine inlet temperature, fan and compressor vane positions as a function of PLA) are defined for the nominal engine. As the engine degrades, these schedules can no longer be achieved.

Degraded-engine performance in conjunction with key control analysis results (Ref. 10) were analyzed. Engine response showed that within 2.5 sec vane positions and high turbine inlet temperature were at their requested values. However, the thrust level was ninety-four percent military thrust (requested value for thrust at PLA = 73 deg is 100 percent military thrust). Analysis of engine inputs showed that the control logic was driving jet exhaust area to its minimum position limit to drive the thrust error (estimated-requested thrust) to zero. Key control analysis indicates that jet exhaust area is a key control input for steady-state as well as transient thrust response.

Degraded-engine performance with the mode-switching logic to accommodate engine degradation was satisfactory. Stochastic degraded and nominal engine

thrust responses are compared in Fig. 7. Figure 7 shows that degraded engine response is only slightly slower than the nominal engine response until 90 percent military thrust is reached (2 sec). The nominal engine reaches 100 percent military thrust at 2.5 sec. On the other hand, the degraded engine does not reach 100 percent military thrust until 5 sec.

The stochastic degraded engine response is compared with deterministic degraded engine response in Fig. 8 (deterministic response is the response achieved by feedback of actual not estimated variables). Figure 8 shows that stochastic and deterministic responses are very similar. Therefore, differences in nominal and degraded engine response with the stochastic controller (that is, the relatively slow degraded-engine thrust response from 90 to 100 percent military thrust) results from degraded engine performance limitations, not from estimation errors in engine variables.

Estimation error statistics (mean and standard deviation) for degraded engine response using the stochastic controller are shown in Table VII. Table VII indicates that very accurate estimates of engine variables are achieved with the nonlinear filtering logic. The absolute average error is 0.002 for fan and high turbine inlet temperature estimates, 0.001 for main burner pressure and fan and compressor stability margin estimates, and zero to three significant figures for all other state and output estimates. The maximum standard deviation is 0.002 in fan turbine inlet temperature; the standard deviation is zero to three significant figures in fan and compressor speed and 0.001 for all other state and output estimates.

Evaluation of degraded engine performance indicates that (1) mode-switching logic to accommodate engine degradation is required for stable, rapid dynamic engine response and (2) model-mismatch compensation within the nonlinear filtering algorithm results in accurate steady-state as well as transient estimation.

Off-Nominal Noise Statistics

The effect of off-nominal noise statistics on stochastic closed-loop engine performance was assessed. Noise-corrupted engine input and measurement data with noise statistics different from those assumed in calculating filter gains were generated for the degraded as well as nominal engine. Standard deviations of the measurement noise were doubled; whereas, fuel flow driving noise standard deviation was halved. Engine response with off-nominal measurement and input noise was the same as engine response with nominal measurement and input noise statistics. (See Fig. 5, stochastic nominal engine and Fig. 7, stochastic degraded engine for thrust response.) These results indicate that the nonlinear stochastic control is insensitive to a mismatch between actual and nominal statistics.

Results obtained in this study show that rapid, stable engine performance is achieved using the stochastic controller with model-mismatch compensation and mode-switching logic. Satisfactory thrust response was achieved with the nonlinear stochastic controller for (1) nominal engine with nominal noise statistics, (2) degraded engine with nominal noise statistics, (3) nominal engine with off-nominal noise statistics, and (4) degraded engine with off-nominal noise statistics. In addition, the controller provided rapid, stable small-signal as well as large-signal dynamic response.

RESULTS AND CONCLUSIONS

1. The nonlinear stochastic feedback control algorithm was interfaced with a nonlinear F100/F401 engine simulation. The overall closed-loop system consists of (1) the nonlinear F100/F401 engine simulation, (2) sensor models, (3) a deterministic piecewise-linear/piecewise-optimal (PLPO) control algorithm with mode-switching logic, and (4) a nonlinear estimator with model-mismatch compensation. Mode-switching logic was developed to provide smooth transition between small-signal and large-signal engine operation. Also, control logic to accommodate engine degradation was defined. Model-mismatch compensation was employed to account for mismatch between the system model within the filtering logic and the actual system model. Engine variables required for feedback through the deterministic control logic include unmeasurable variables (thrust and high turbine inlet temperature) as well as measured variables (fan and compressor speeds, main burner and afterburner pressures, and fan turbine inlet temperature). The nonlinear stochastic controller (deterministic PLPO control/nonlinear estimator) was evaluated throughout the idle to military sea-level static operating regime (9 to 100 percent thrust).

   (a) Closed-loop engine/control/filter stability-in-the-small as well as stability-in-the-large was assessed at design and off-design operating points. Stability-in-the-small at design points is assured under appropriate assumptions using the design procedures employed in this study. Stability-in-the-small at off-design operating conditions was demonstrated from computation of closed-loop system eigenvalues at selected off-design operating conditions. Stability-in-the-large was shown through computer simulation.

   (b) Small-signal engine performance using control logic with and without mode-switching logic was compared. Small-signal thrust response with mode-switching logic incorporated into the controller was significantly faster than thrust response without mode-switching logic. Also, mode-switching logic provided a smooth transition between small- and large-signal operation.

   (c) Nominal stochastic engine performance (nominal engine model/control/estimator/nominal fuel flow and measurement uncertainties) was compared with nominal deterministic engine performance (nominal engine model/control/no estimator or system uncertainties). Stochastic thrust response was as rapid as deterministic thrust response for both large- and small-signal operation. Stochastic engine response of other critical variables was very similar to the deterministic response. This similarity in deterministic and stochastic performance was achieved by assuring that neither control nor estimator dynamics were dominant.

(d) The stochastic control algorithm was also evaluated by application to a degraded F100/F401 engine simulation. Engine degradation was achieved through decreases in fan and compressor efficiencies representative of realistic operating conditions. Stochastic degraded engine response was slower than nominal engine response. Comparison of stochastic and deterministic engine performance shows that the slower degraded engine response results from degraded engine performance limitations rather than from estimation errors in engine variables.

(e) Performance of the stochastic control algorithm was evaluated for measurement and fuel flow metering noise statistics different from those assumed in the design procedure. Engine response with off-nominal noise was the same as the response with nominal noise. That is, the closed-loop system response was insensitive to a realistic mismatch in actual and assumed noise statistics.

2. Results obtained indicate that the nonlinear stochastic controller design procedures employed herein provide a viable approach for gas turbine control design.

(a) Stability-in-the-small and in-the-large was established. Rapid, stable thrust response was achieved (1) for small-signal as well as large-signal operation, (2) for a nominal engine model, (3) for a degraded engine model, and (4) for off-nominal noise statistics.

(b) Computational requirements for the stochastic controller depend upon (1) control gain calculations, (2) control computations to update engine inputs, (3) filter gain calculations, and (4) the engine model employed in the filter. The control and filter gain calculations as well as the input update calculations require only 154 multiplications and 271 additions per sampling interval. A minimum complexity engine model should be selected for the filtering algorithm to reduce model computational requirements. Model-mismatch compensation logic should be employed to compensate for differences between the engine model in the filter and the actual engine.

RECOMMENDATIONS FOR FUTURE STUDY

Results of this study indicate that a multivariable stochastic controller designed using modern state-space estimation and control techniques is a feasible approach to control of complex, nonlinear variable geometry gas turbine engines. Studies that represent a logical broadening and analytical extension of the research reported herein are:

- Exhaust gas reingestion: Apply the control and estimation methodology developed in this study to define and evaluate control and estimation logic necessary to maintain thrust during reingestion of engine exhaust gases. Problems resulting from hot gas ingestion assume increasingly greater importance as the Navy focuses its attention upon future large-scale deployment of high-speed tactical V/STOL aircraft.

- Hybrid evaluation: Evaluate the nonlinear stochastic controller on a real-time detailed F100/F401 hybrid simulation. The control law would be coded on a digital minicomputer. Hardware requirements, system accuracy, stability as a function of sampling rate, and control computation time would be delineated. This evaluation would be directed toward eventual engine test of the stochastic controller.

- Diagnostics: Develop and evaluate diagnostic algorithms for predicting and identifying engine degradation using the nonlinear estimator. The nonlinear estimator with model-mismatch compensation achieves accurate estimates of degraded engine variables. Power spectral analysis of the error between estimated variables and nominal steady-state values could be employed to identify engine degradation. Results of the analyses could be employed for maintenance scheduling. In addition, adaptive modulation of control gains based on the amount of identified degradation could be employed to achieve rapid, safe acceleration as well as accurate steady-state regulation despite engine degradation.

- Performance-seeking logic: UTRC studies carried out under NSF support (Ref. 4) have resulted in successful development of adaptive control logic for in-flight minimization of thrust specific fuel consumption (TSFC). The developed performance-seeking algorithm was evaluated on the F100/F401 engine simulation (Ref. 7) using actual, not estimated variables. The nonlinear estimator described herein provides a potential means for estimating unmeasurable engine variables for use within the performance-seeking logic. A program should be conducted to interface the estimator with the developed TSFC in-flight optimization algorithm. TSFC improvements over a range of representative flight conditions should then be determined.

REFERENCES

1. Clark, J. W., Jr.: Analysis of Response Requirements for V/STOL Lift/Cruise Engines Used to Provide Height and Moment Control. AIAA 1975 Aircraft Systems and Technology Meeting, August 1975.

2. Michael, G. J. and F. A. Farrar: Development of Optimal Control Modes for Advanced Technology Propulsion Systems. United Aircraft Research Laboratories Report M911620-1, Interim Technical Report prepared under Department of the Navy Contract N00014-73-C-0281, August 1973 (DDC Accession No. AD 767425).

3. Michael, G. J. and F. A. Farrar: Development of Optimal Control Modes for Advanced Technology Propulsion Systems. United Aircraft Research Laboratories Report N911620-2, Annual Technical Report prepared under Department of the Navy Contract N00014-73-C-0281, March 1974 (DDC Accession No. AD 775337).

4. Jordan, D. and G. J. Michael: Development of Gas Turbine Performance Seeking Logic. ASME Publication No. 78-GT-13, presented at the ASME International Gas Turbine Conference, London, England, April 9-13, 1978.

5. Michael, G. J. and F. A. Farrar: An Analytical Method for the Synthesis of Nonlinear Multivariable Feedback Control. United Aircraft Research Laboratories Report M941338-2, Final Technical Report prepared under Department of the Navy Contract N00014-72-C-0414, June 1973 (DDC Accession No. AD 762797).

6. Farrar, F. A. and G. J. Michael: Large-Signal Estimation for Stochastic Nonlinear Multivariable Dynamic Systems. Office of Naval Research Report ONR-CR215-247-1, Annual Technical Report prepared under Department of the Navy Contract N00014-76-C-0710, March 1977 (DDC Accession No. AD 040901).

7. Anon: F100-PW-100 (F100/F401) Digital Dynamic Simulation User's Manual for Deck CCD 1015-3.2, Book 1 of 2. Pratt & Whitney Aircraft Report PWA FR-3794B, prepared under Department of the Air Force Contract F33657-70-C-0600, October 15, 1970, revised April 25, 1972.

8. Michael, G. J. and F. A. Farrar: Stochastic Regulation of Nonlinear Multivariable Dynamic Systems. Office of Naval Research Report ONR-CR215-219-4F, Final Technical Report prepared under Department of the Navy Contract N00014-73-C-0281, March 1976 (DDC Accession No. AD-A-021451).

REFERENCES (Continued)

9. Michael, G. J. and F. A. Farrar: Identification of Multivariable Gas Turbine Dynamics from Stochastic Input-Output Data. United Aircraft Research Laboratories Report R941620-3, Annual Technical Report prepared under Department of the Navy Contract N00014-73-C-0281, March 1975 (DDC Accession No. AD A006277).

10. Michael, G. J. and G. S. Sogliero: Key Control Assessment for Linear Multivariable Systems. United Technologies Research Center Report R76-942042, Final Technical Report prepared under Department of the Air Force Contract F44620-75-C-0027, January 1976.

LIST OF SYMBOLS

A_e	Constant 5x5 matrix used to describe linearized engine dynamics
A_j	Jet exhaust area, normalized
A_τ	5x5 matrix used to represent sensor dynamics
$(A_\tau)_{ij}$	Element in the i^{th} row and j^{th} column of the matrix A_τ
B_e	Constant 5x4 matrix used to describe linearized engine dynamics
C_e	Constant 5x5 matrix used to describe linearized engine dynamics
D_e	Constant 5x4 matrix used to describe linearized engine dynamics
e_1	5x1 error vector used to represent the difference between actual and estimated engine state perturbations
e_2	5x1 error vector used to represent the difference between sensed and estimated sensor state perturbations
F_{11}	Constant 9x9 matrix used to represent engine control dynamics
F_{22}	Constant 5x5 matrix used to represent sensor dynamics
F_{33}	Constant 15x15 matrix used to represent stochastic estimator dynamics
f_1	Nonlinear 5x1 vector function -- mathematical representation of rate-of-change of reduced order engine state vector
g	Nonlinear 5x1 vector function -- mathematical representation of engine output vector
g_{ke}	General gain
H	4x4 optimal integral feedback regulator gain matrix
H_c	$H\Delta t$
I_5	5x5 identity matrix
K	Amplification gain in mode-switching logic
K_1	Component of mode-switching logic gain -- function of thrust error

K_2	Component of mode-switching logic gain -- function of high turbine inlet temperature
K_c	5x5 compensator gain matrix for estimator with model-mismatch compensation
K_{f_1}	5x5 upper partition of Kalman filter gain matrix for estimator with model-mismatch compensation
K_{f_2}	5x5 lower partition of Kalman filter gain matrix for estimator with model-mismatch compensation
L	4x5 optimal integral feedback regulator gain matrix
m	Slope associated with linear gain interpolation
N_2	High compressor speed, normalized
O_{ij}	ixj null matrix
PLA	Power lever angle, degrees
t	time, sec
Δt	Sample time, sec
u	4x1 control vector
v	4x1 vector used to represent engine variables whose steady-state values are specified
v_c	4x1 vector used to represent the commanded values of v
w	5x1 vector used to represent filter model-mismatch
x	10x1 system state vector
x_e	5x1 engine state vector
x_e^+	16x1 engine state vector
x_s	5x1 sensor state vector
y	5x1 engine output vector

LIST OF SYMBOLS (Continued)

z	5x1 engine measurement vector
$\delta(\ )$	Perturbational value of quantity in parenthesis
η	5x1 sensor noise vector
ξ	4x1 actuator (process) noise vector
τ_i	Sensor time constant associated with the i^{th} engine state
$(\hat{\ })$	Estimated value of quantity in parenthesis
$(\dot{\ })$	Time derivative of quantity in parenthesis
$d(\ )$	Differential of quantity in parenthesis
$\Delta(\ )$	Finite increment of quantity in parenthesis
$\underline{\Delta}$	Equals by definition

TABLE I

NORMALIZED STEADY-STATE ENGINE PARAMETERS
AS FUNCTIONS OF POWER LEVER ANGLE
Sea-Level Static Operating Condition
Idle Condition: PLA = 20 deg
Military Condition: PLA = 73 deg

Engine Parameters		Power Lever Angle, PLA-deg				
Type	Parameter	20	35	47	60	73
Output	Fan Airflow	0.34	0.62	0.73	0.85	1.0
	Fan Stability Margin	0.10	0.14	0.18	0.12	0.12
	Compressor Stability Margin	0.16	0.18	0.18	0.19	0.19
	Thrust	0.09	0.35	0.52	0.72	1.0
	High Turbine Inlet Temperature	0.56	0.73	0.81	0.90	1.0
State	Fan Turbine Inlet Temperature	0.57	0.72	0.81	0.90	1.0
	Main Burner Pressure	0.21	0.45	0.59	0.77	1.0
	Fan Speed	0.49	0.74	0.83	0.91	1.0
	Compressor Speed	0.69	0.83	0.88	0.93	1.0
	Afterburner Pressure	0.40	0.55	0.66	0.82	1.0
Control	Jet Exhaust Area	0.98	0.98	0.98	0.98	1.0
	Fan Inlet Guide Vanes	-0.50	-0.50	-0.50	-0.34	-0.08
	Compressor Variable Vanes	-1.11	-0.39	-0.17	0.04	0.20
	Main Burner Fuel Flow	0.12	0.33	0.48	0.70	1.0

TABLE II

NOISE STATISTICS AND SENSOR TIME CONSTANTS

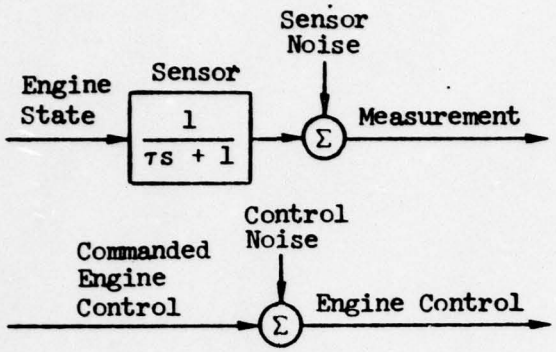

Variable Type	Variable	Sensor Time Constant (τ, sec)	Normalized Standard Deviation of Noise
Measurement	Fan Turbine Inlet Temperature	1.50	0.75×10^{-2}
	Main Burner Pressure	0.10	0.10×10^{-1}
	Fan Speed	0.03	0.15×10^{-2}
	Compressor Speed	0.05	0.11×10^{-2}
	Afterburner Pressure	0.10	0.10×10^{-1}
Control	Jet Exhaust Area	-	0
	Fan Inlet Guide Vanes	-	0
	Compressor Variable Vanes	-	0
	Main Burner Fuel Flow	-	1% of Commanded Fuel Flow

TABLE III

DESIGN POINT F100/F401 CLOSED-LOOP SYSTEM EIGENVALUES

Power Lever Angle = 73 Deg

Eigenvalues Associated With					
Sensor Dynamics		Deterministic Control Mode		Estimator	
Real	Imaginary	Real	Imaginary	Real	Imaginary
-33.333	0	-33.058	-1.041	-35.876	-6.884
-20.0	0	-33.058	1.041	-35.876	6.884
-10.0	0	-5.642	-1.112	-29.570	0
-10.0	0	-5.642	1.112	-18.991	0
-0.667	0	-4.516	0	-10.670	0
		-3.361	0	-10.245	0
		-1.862	-1.351	- 9.942	-10.873
		-1.862	1.351	- 9.942	10.873
		-1.293	0	- 7.425	-6.118
				- 7.425	6.118
				- 3.781	-3.437
				- 3.781	3.437
				- 0.577	-0.171
				- 0.577	0.171
				- 0.297	0

TABLE IV

ERROR INDICES ASSOCIATED WITH LINEAR
F100/F401 ENGINE MODELS

$$\text{ERROR INDEX} \triangleq \left[\frac{\sum_{i=1}^{N} (\text{ACTUAL RESPONSE} - \text{IDENTIFIED RESPONSE})^2}{\sum_{i=1}^{N} (\text{ACTUAL RESPONSE})^2} \right]^{1/2}$$

N = Number of Data Points

Variable Type	Variable	PLA (deg) 28	41	54	67
State	Fan Turbine Inlet Temperature	0.048	0.045	0.106	0.152
	Main Burner Pressure	0.038	0.038	0.085	0.191
	Fan Speed	0.017	0.019	0.034	0.065
	Compressor Speed	0.029	0.038	0.047	0.047
	Afterburner Pressure	0.029	0.026	0.037	0.072
Output	Fan Corrected Airflow	0.015	0.018	0.030	0.167
	Fan Stability Margin	0.111	0.040	0.070	0.116
	Compressor Stability Margin	0.106	0.156	0.183	0.290
	Thrust	0.024	0.024	0.016	0.018
	High Turbine Inlet Temperature	0.034	0.033	0.034	0.032

TABLE V

OFF-DESIGN POINT F100/F401 CLOSED-LOOP SYSTEM EIGENVALUES

Power Lever Angle = 67 Deg

Eigenvalues Associated With					
Sensor Dynamics		Deterministic Control Mode		Estimator	
Real	Imaginary	Real	Imaginary	Real	Imaginary
-33.333	0	-38.933	0	-44.178	0
-20.0	0	-20.082	8.945	-34.210	0
-10.0	0	-20.082	-8.945	-21.567	0
-10.0	0	- 5.029	0	-15.958	0
- 0.667	0	- 3.568	3.068	-11.698	8.002
		- 3.568	-3.068	-11.698	-8.002
		- 2.375	0.683	- 7.644	2.194
		- 2.375	-0.683	- 7.644	-2.194
		- 0.824	0	- 6.552	12.040
				- 6.552	-12.040
				- 2.720	0
				- 1.263	0
				- 0.896	1.185
				- 0.896	-1.185
				- 0.378	0

TABLE VI

F100/F401 ESTIMATION ERROR STATISTICS ASSOCIATED WITH NOMINAL ENGINE

Estimation Error $\triangleq$ Actual-Estimated Response

Variable Type	Variable	Average Error	Standard Deviation of Error
State	Fan Turbine Inlet Temperature	0.000	0.002
	Main Burner Pressure	0.000	0.001
	Fan Speed	0.000	0.000
	Compressor Speed	0.000	0.000
	Afterburner Pressure	0.000	0.001
Output	Fan Corrected Airflow	0.000	0.000
	Fan Stability Margin	0.000	0.001
	Compressor Stability Margin	0.000	0.001
	Thrust	0.000	0.001
	High Turbine Inlet Temperature	0.000	0.001

TABLE VII

F100/F401 ESTIMATION ERROR STATISTICS ASSOCIATED WITH DEGRADED ENGINE

Estimation Error $\triangleq$ Actual-Estimated Response

Variable Type	Variable	Average Error	Standard Deviation of Error
State	Fan Turbine Inlet Temperature	0.002	0.002
	Main Burner Pressure	-0.001	0.001
	Fan Speed	0.000	0.000
	Compressor Speed	0.000	0.000
	Afterburner Pressure	0.000	0.001
Output	Fan Corrected Airflow	0.000	0.001
	Fan Stability Margin	-0.001	0.001
	Compressor Stability Margin	-0.001	0.001
	Thrust	0.000	0.001
	High Turbine Inlet Temperature	0.002	0.001

CLOSED–LOOP FEEDBACK CONTROL STRUCTURE

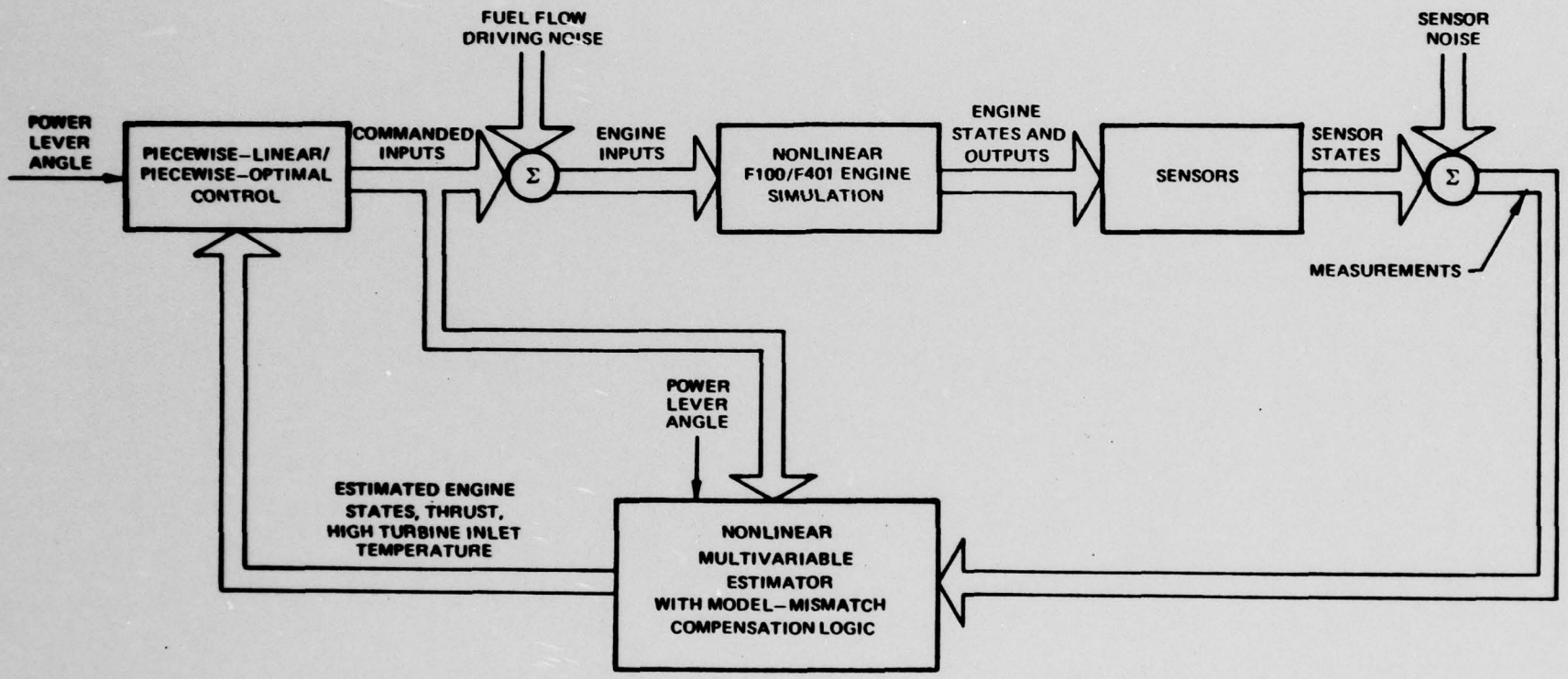

FIG. 1

NORMALIZED F100/F401 ENGINE MODEL STATE RESPONSES WITH LARGEST AND SMALLEST ERROR INDICES

POWER LEVER ANGLE = 67 DEG

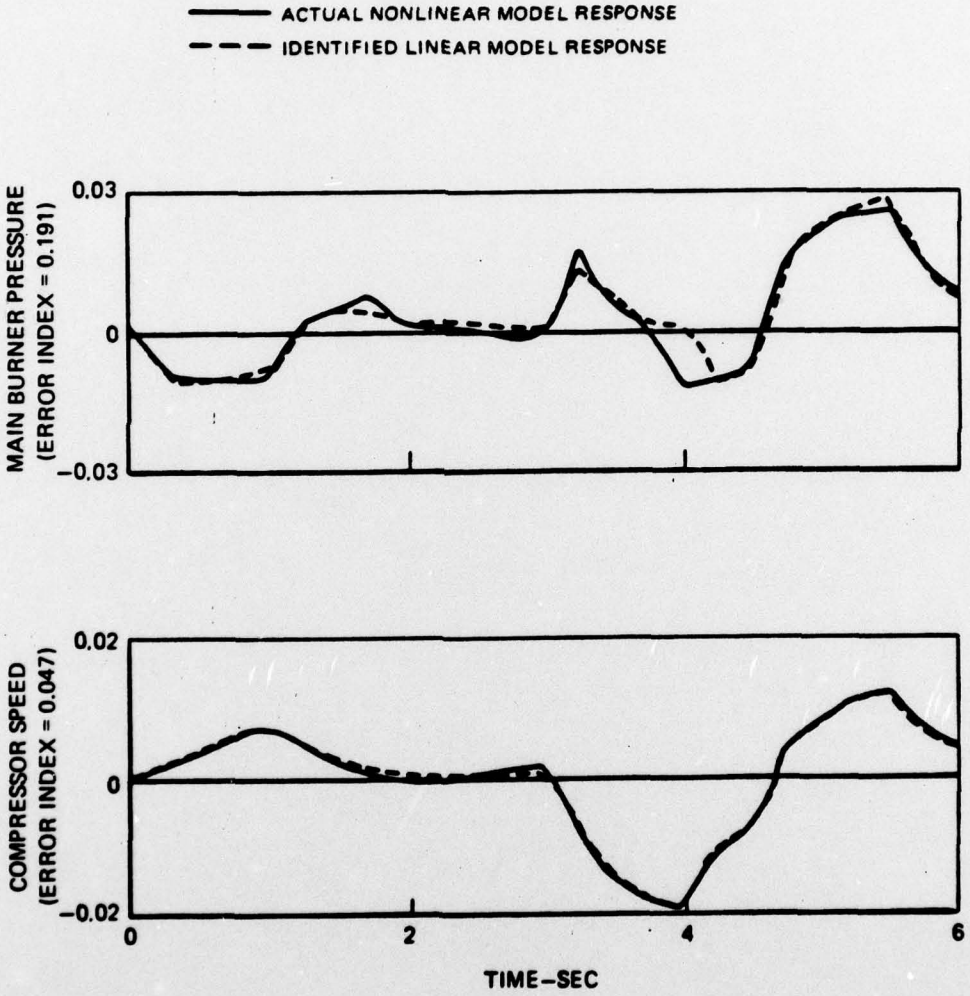

77-10-83-1

FIG. 3

NORMALIZED F100/F401 ENGINE MODEL OUTPUT RESPONSES WITH LARGEST AND SMALLEST ERROR INDICES

POWER LEVER ANGLE = 67 DEG

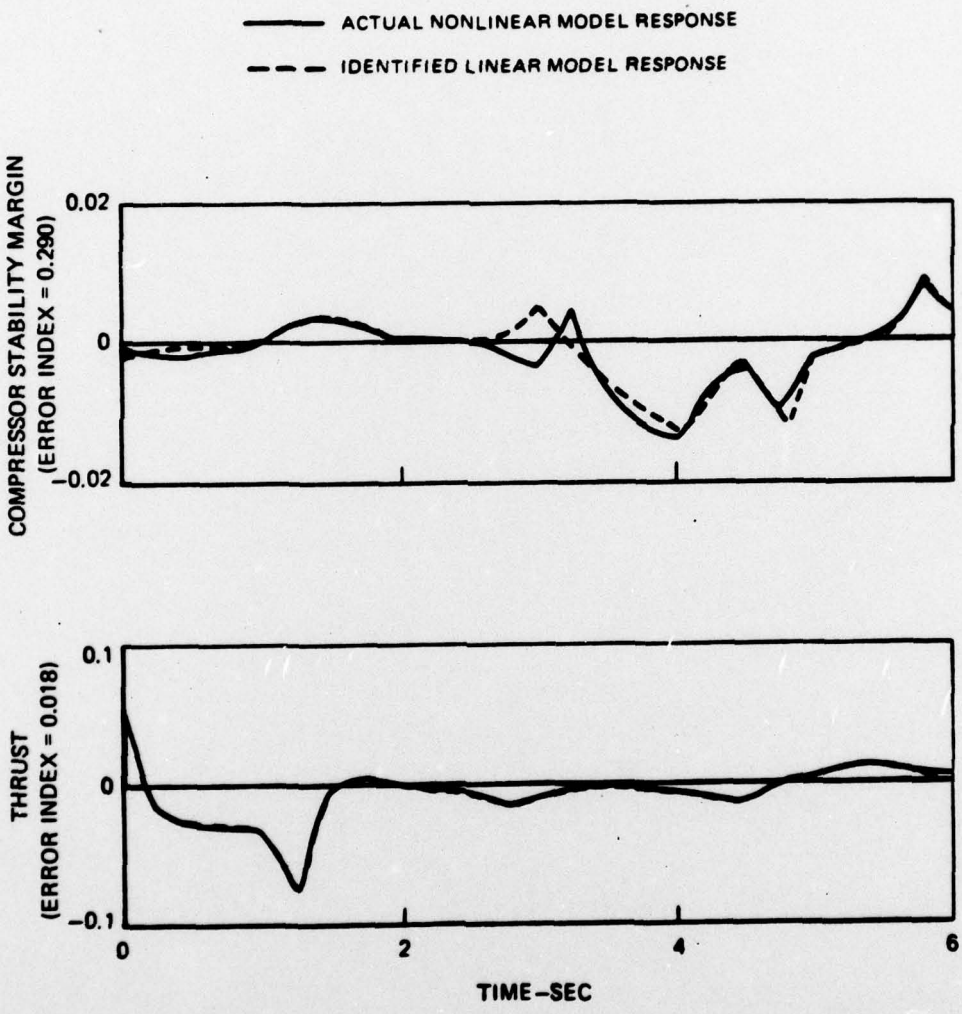

77-10-83-2

MODE–SWITCHING LOGIC TO ACHIEVE RAPID SMALL–SIGNAL RESPONSE

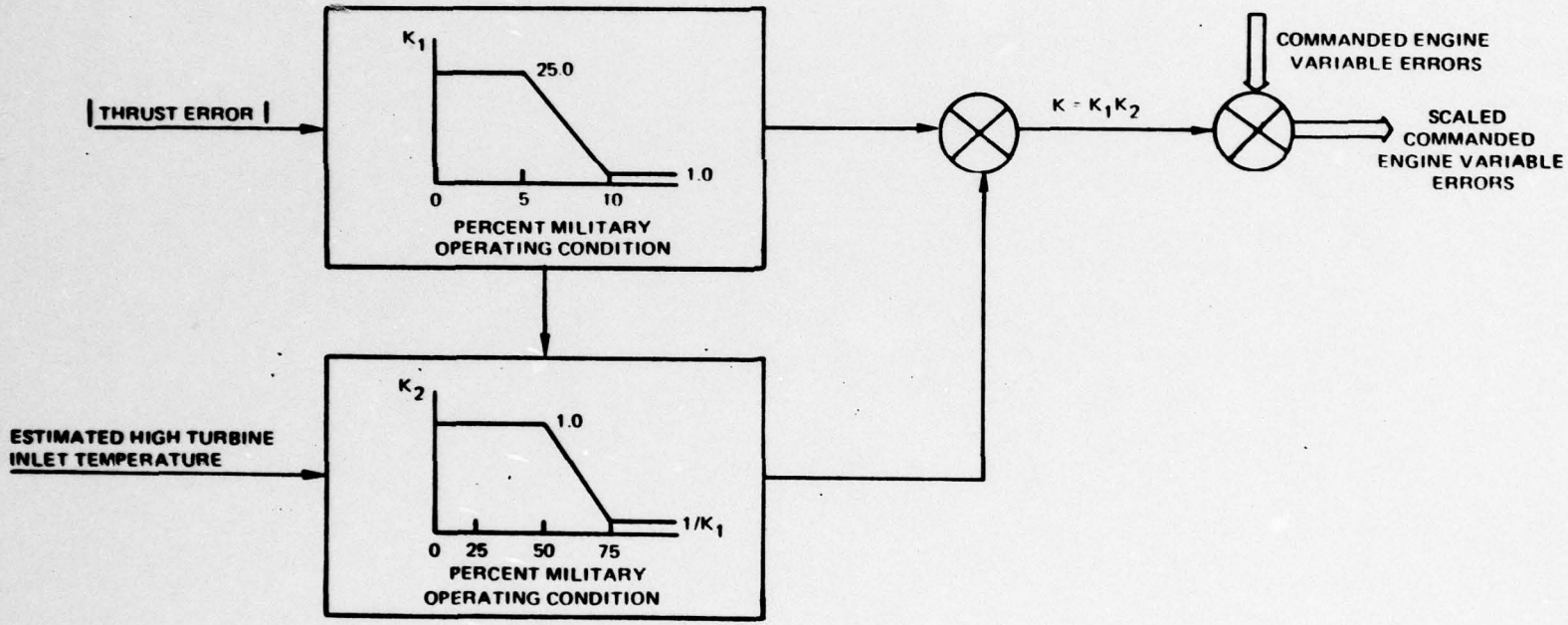

77-12-90-2

FIG. 4

FIG. 5

COMPARISON OF NORMALIZED STOCHASTIC AND DETERMINISTIC NOMINAL F100/F401 THRUST RESPONSE

IDLE TO MIL TRANSIENT

——— DETERMINISTIC CLOSED–LOOP SYSTEM RESPONSE

– – – STOCHASTIC CLOSED–LOOP SYSTEM RESPONSE

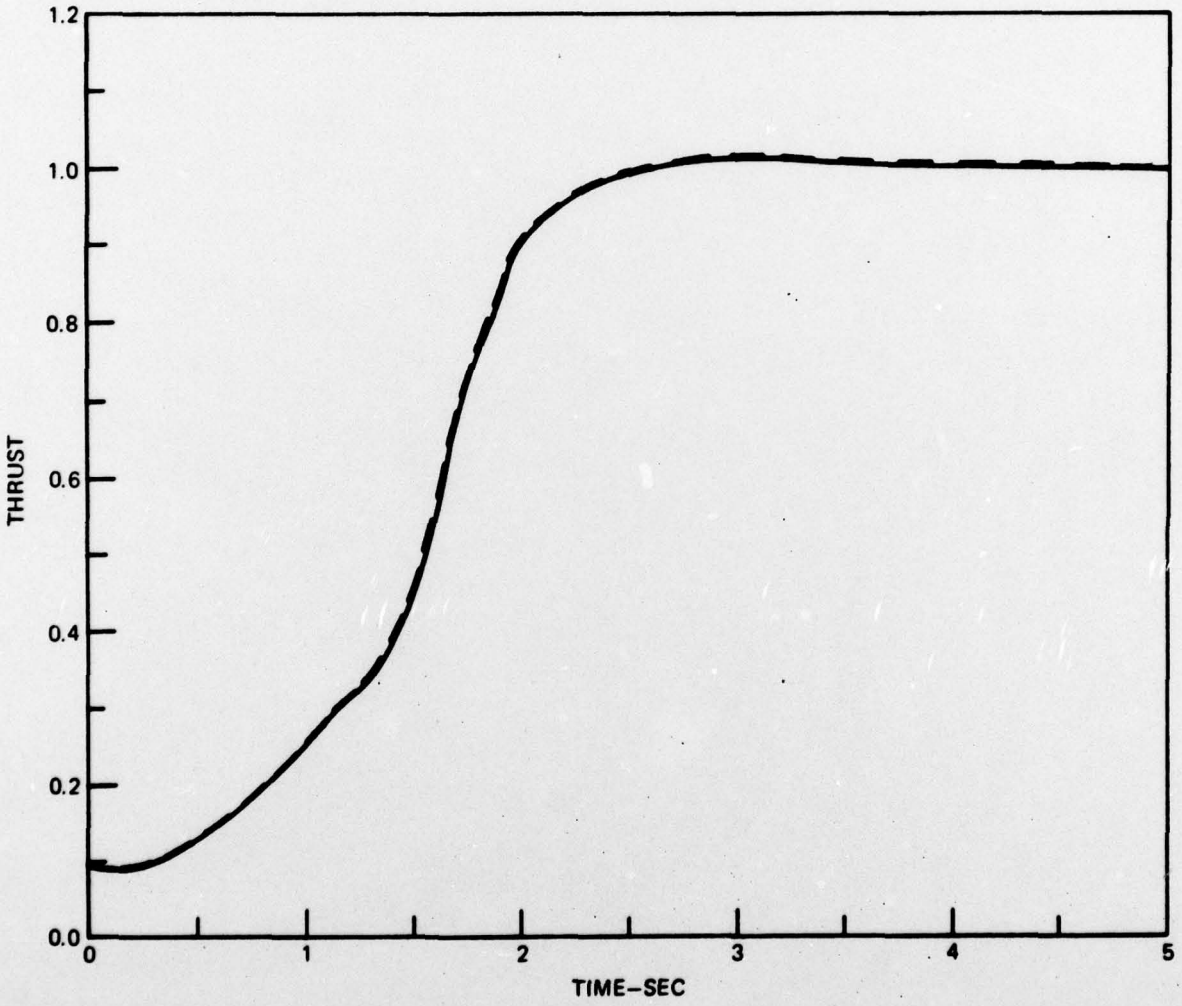

78–05–78–3

FIG. 6

NORMALIZED STOCHASTIC NOMINAL F100/F401 SMALL–SIGNAL THRUST RESPONSE

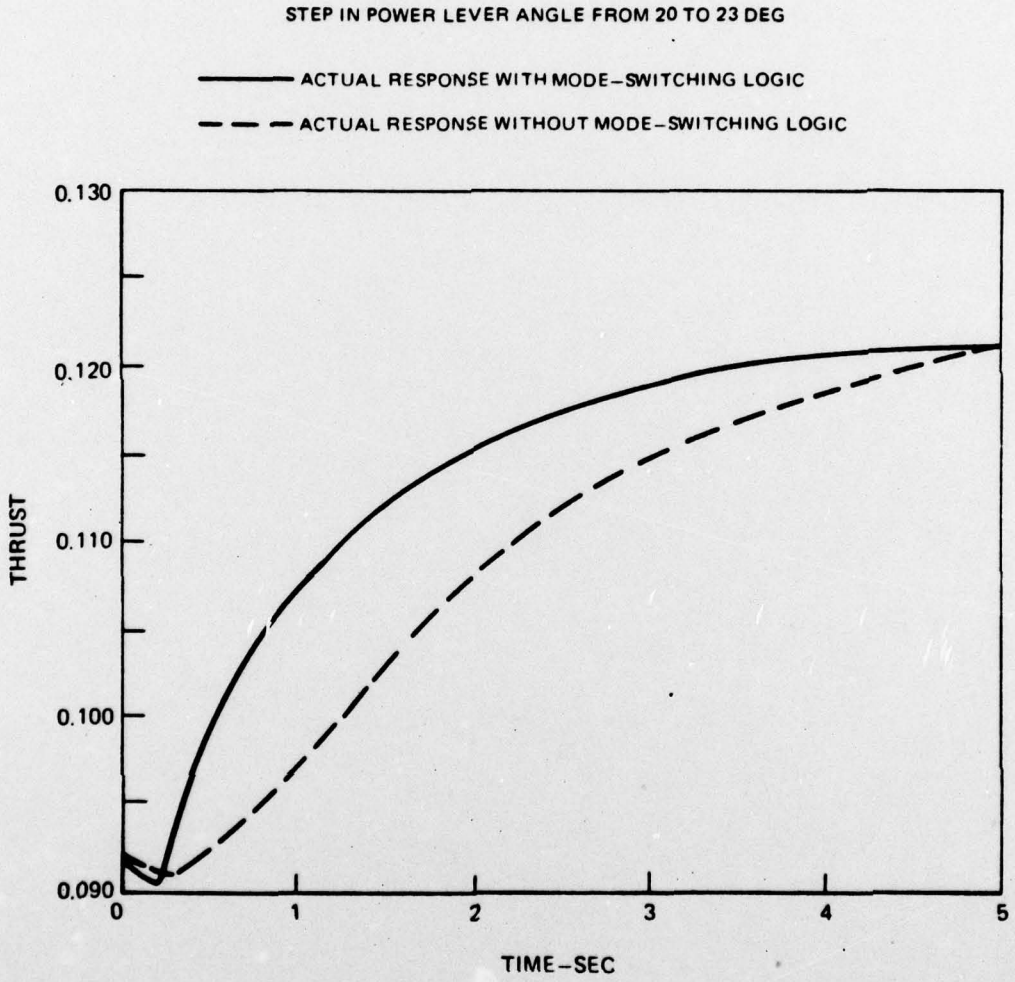

77–12–90–1

FIG. 7

COMPARISON OF NORMALIZED STOCHASTIC DEGRADED AND NOMINAL F100/F401 THRUST RESPONSE

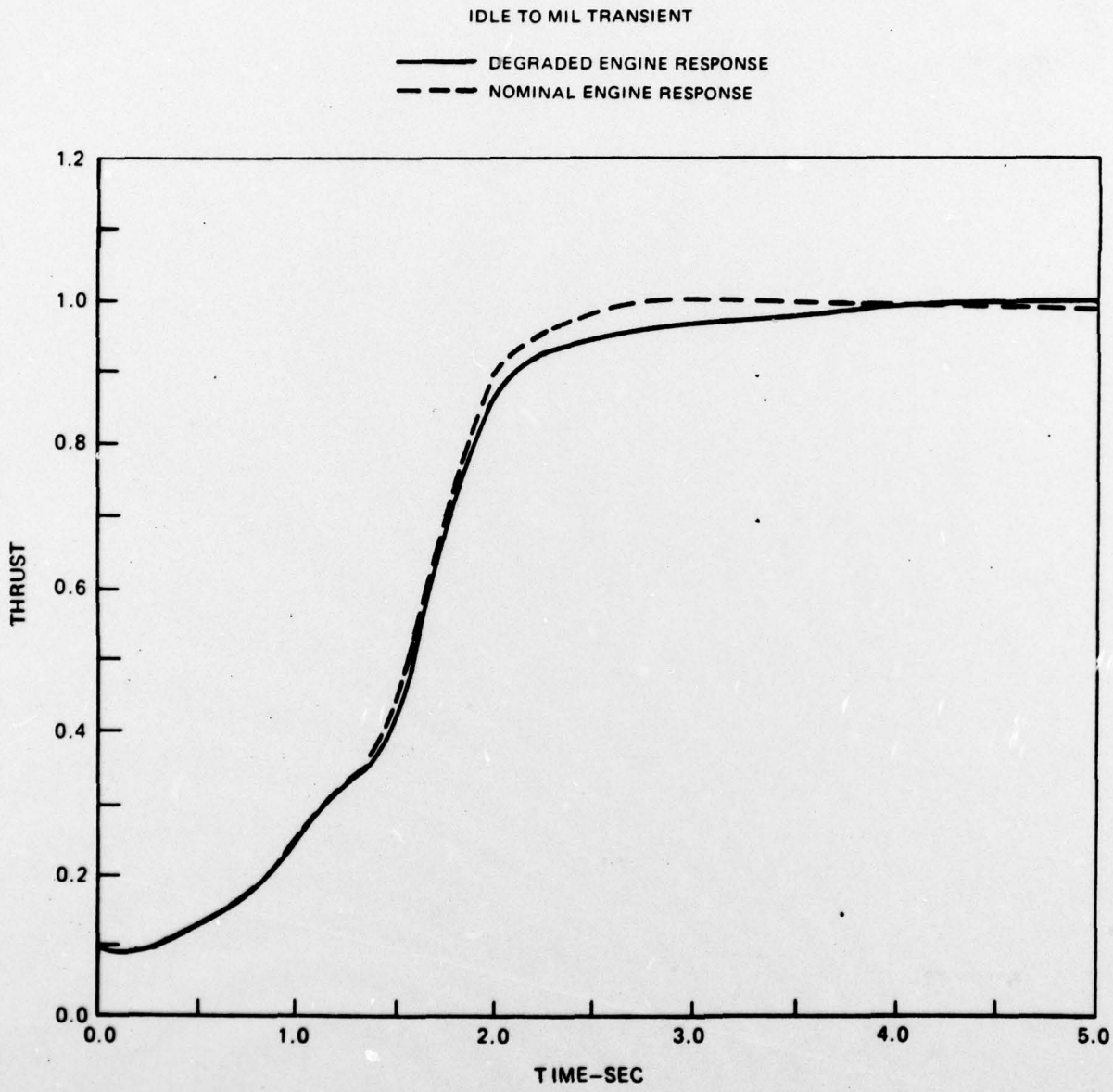

78–05–78–5

FIG. 8

COMPARISON OF NORMALIZED STOCHASTIC AND DETERMINISTIC DEGRADED F100/F401 THRUST RESPONSE

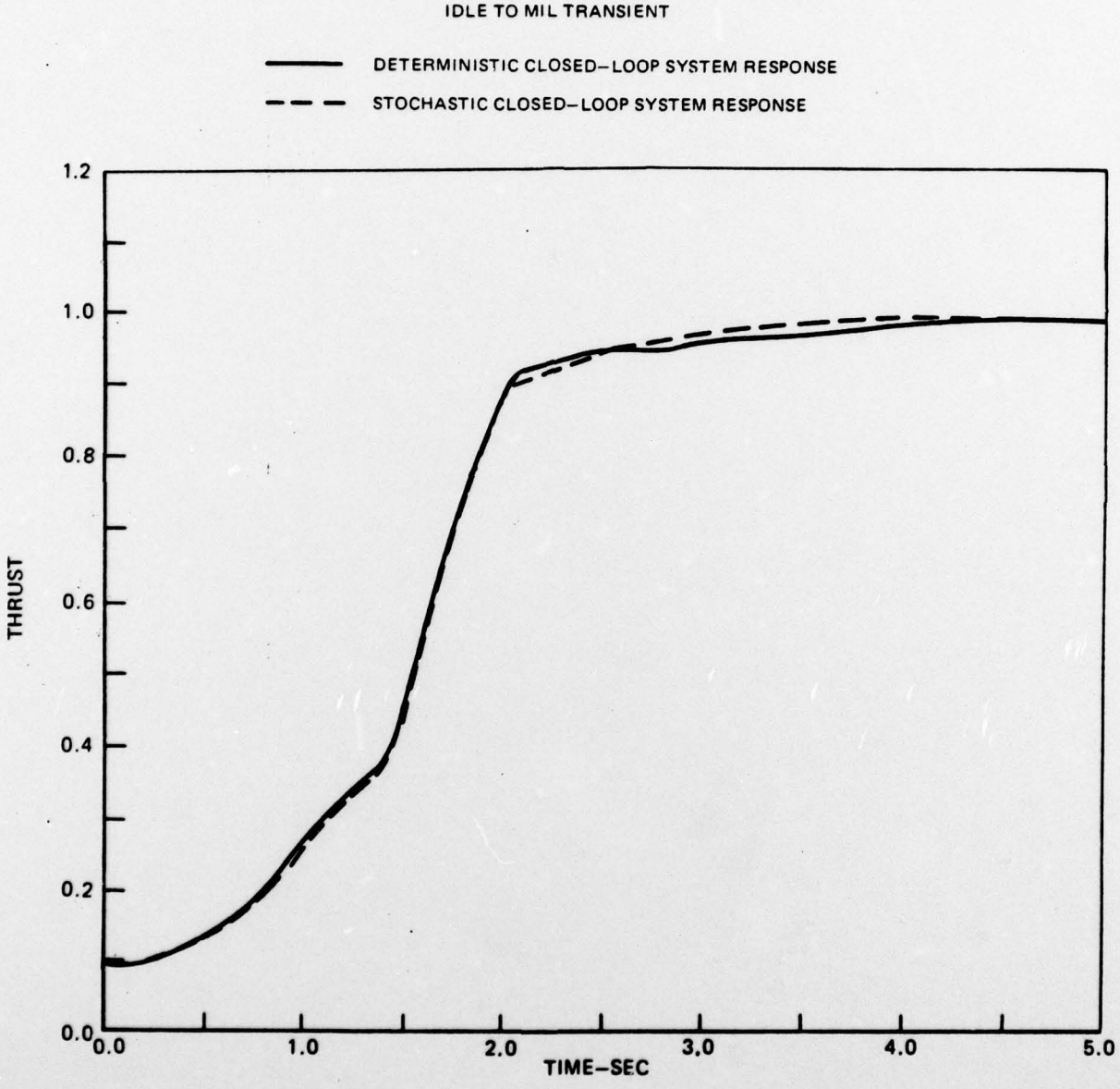

78–05–78–4

DISTRIBUTION LIST

Office of Naval Research
800 N. Quincy Street
Arlington, VA 22217
- R. von Husen, Code 211 — 4
- S. L. Brodsky, Code 432 — 1
- J. R. Patton, Code 473 — 1

Office of Naval Research
Branch Office
495 Summer Street
Boston, MA 02210 — 1

Office of Naval Research
Branch Office
715 Broadway - 5th Floor
New York, NY 10003 — 1

Naval Research Laboratory
Washington, DC 20375
- Code 2627 — 3

Naval Air Systems Command
Washington, DC 20361
- R. R. Brown, AIR 330 — 1
- A. J. Schmidt, AIR 5363 — 1

Naval Air Propulsion Center
Trenton, NJ 08628
- A. A. Martino, Dept. PE — 1
- D. F. Brunda, Dept. PE — 1
- B. A. Barclay, Dept. PE — 1
- R. T. Lazarick, Dept. PE — 1

Naval Air Development Center
Warminster, PA 18974
- A. G. Piranian, Code 6072 — 1
- Technical Reports Library — 1

Naval Material Command
Washington, DC 20360
- Code 08T23 — 1

Naval Weapons Center
China Lake, CA 93555
- Technical Report Library — 1

Naval Avionics Facility
21st and Arlington Ave.
Indianapolis, IN 46218
- Technical Report Library — 1

Naval Post Graduate School
Monterey, CA 93940
- Technical Reports Library — 1

Defense Documentation Center
Building 5
Cameron Station
Alexandria, VA 22314 — 12

Air Force Plant Representative Office
Pratt & Whitney Aircraft
East Hartford, CT 06108
- W. McAvoy — 1

Air Force Office of Scientific Research
Building 410
Bolling Air Force Base
Washington, DC 20332
- Maj. C. L. Nefzger — 1

Air Force Aero Propulsion Laboratory
Wright-Patterson Air Force Base
Dayton, OH 45433
- C. E. Bentz — 1
- L. L. Small — 1
- C. A. Skira — 1

NASA Lewis Research Center
Cleveland, OH 44135
- D. Drain — 1
- D. Cwynar — 1
- B. Lehtinen — 1
- J. Zeller — 1

NASA Langley Research Center
Hampton, VA 23665
- R. J. Tapscott — 1

Systems Control Inc.
1801 Page Mill Road
Palo Alto, CA 94306
- E. Hall — 1

The Analytic Sciences Corp.
6 Jacob Way
Reading, MA 01867
- C. Price — 1

Calspan Corp.
P. O. Box 400
Buffalo, NY 14225
- E. G. Rynaski — 1

Honeywell, Inc.
Systems and Research Center
2600 Ridgway Parkway N.E.
Minneapolis, MN 55413
C. A. Harvey 1